Original article

A quantitative enhancement characterization of hyperfunctioning parathyroid lesions on four-dimensional CT scans

Netsiri Dumrongpisutikul*, Ornalin Boonsirisak

Department of Radiology, Faculty of Medicine, King Chulalongkorn Memorial Hospital, Thai Red Cross Society, Bangkok, Thailand

Background: Approximately 20.0% of hyperfunctioning parathyroid lesions do not exhibit typical enhancement characteristics on Four-dimensional computed tomography (4DCT). The two main mimics of hyperfunctioning parathyroid lesions are thyroid tissue and lymph nodes.

Objective: The study aimed to characterize enhancement patterns of hyperfunctioning parathyroid lesions on four-dimensional computed tomography (4DCT) and to differentiate hyperfunctioning parathyroid lesions from thyroid gland and lymph node.

Methods: This retrospective study included analysis of 47 hyperfunctioning parathyroid lesions either pathologically proven or uptake on Tc99m-sestamibi SPECT-CT. The attenuation of hyperfunctioning parathyroid lesions, thyroid glands, lymph nodes and muscles at non-contrast, arterial phase and delayed phase were measured. The discriminant function and optimal cut-off value were evaluated using receiver operating characteristic (ROC) curve analysis. Subgroup analysis between all included lesions and exclusively pathologically proven lesions were performed.

Results: Hyperfunctioning parathyroid lesions showed significantly lower attenuation than thyroid glands in all phases ($P < 0.001$) and significantly higher arterial uptake percentage, delayed uptake percentage and washout percentage than thyroid glands. The area under the ROC curve was greatest in the non-contrast phase, with an optimal cut-off value of ≤ 71.7 hounsfield units (HU) in both subgroups. Hyperfunctioning parathyroid lesions showed significantly higher attenuation than lymph nodes in the arterial and delayed phases and significantly higher arterial uptake and washout percentage than lymph nodes. The area under the ROC curve was greatest in the arterial phase, with an optimal cut-off value of ≥ 107.1 HU in both subgroups.

Conclusion: The best single phase to differentiate hyperfunctioning parathyroid lesions from thyroid glands and lymph nodes were non-contrast and arterial phases, respectively. Arterial uptake percentage was the best discriminator between hyperfunctioning parathyroid lesions from thyroid glands and lymph nodes, as hyperfunctioning parathyroid lesions showed a significantly higher uptake percentage.

Keywords: Hyperfunctioning parathyroid lesion, 4DCT, multidetector computed tomography.

Hyperparathyroidism (HPT) is characterized by abnormally high parathyroid hormone levels in the blood due to overactivity of the parathyroid glands. It is differentiated into three types based on the underlying cause: primary hyperparathyroidism, secondary hyperparathyroidism and tertiary hyperparathyroidism.[1]

*Correspondence to: Netsiri Dumrongpisutikul,
Department of Radiology, Faculty of Medicine, King Chulalongkorn Memorial Hospital, Thai Red Cross Society, Bangkok 10330, Thailand.
E-mail: Netsiri.d@chula.ac.th
Received: March 3, 2022
Revised: May 15, 2022
Accepted: July 25, 2022

Surgical resection of abnormal parathyroid tissue is the primary treatment option for primary and tertiary hyperparathyroidism. Since 2000, a more focused approach or minimally invasive parathyroidectomy performed by resection of abnormal tissue through a small incision has been widely adopted.[2 - 4] Successful preoperative localization of abnormal parathyroid tissue is essential for this less invasive operation.[5]

Imaging modalities for preoperative localization of hyper-functioning parathyroid tissue are technetium-99m sestamibi single-positron emission computed tomography (SPECT), ultrasound and Four-dimensional computed tomography (4DCT).[6 - 8]

Tc99m-sestamibi SPECT is the primary and standard method used for preoperative localization of parathyroid adenoma. The disadvantage of Tc99m-sestamibi SPECT is the limited spatial resolution in the setting of small adenomas. Ultrasound is an operator dependent procedure which has limitations in detecting heterotopic parathyroid adenomas in obese patients and patients with multinodular goiters.[8]

The most recent imaging modality is 4DCT. 4D-CT is multi-detector CT image acquisition at two or more time points before and after the intravenous contrast administration, providing physiologic information of tissue.[9 - 12] Hyperfunctioning parathyroid lesions are typically iso-attenuating to muscle and have lower attenuation than the iodine-containing thyroid before administration of contrast, hyper-enhancement during in arterial phase (A phase) and rapid washout of contrast in the delayed phase (D phase). However, approximately 20.0% of hyperfunctioning parathyroid lesions do not exhibit typical enhancement characteristics. The two main mimics of hyperfunctioning parathyroid lesions are thyroid tissue and lymph nodes.

There are several studies about enhancement patterns of hyperfunctioning parathyroid lesions comparing them with thyroid tissue and lymph nodes. However, variable enhancement patterns have been described. [13 - 20]

The purpose of this study was to characterize enhancement patterns of hyperfunctioning parathyroid lesions on 4DCT and to differentiate hyperfunctioning parathyroid lesions from thyroid tissue and lymph nodes.

Materials and methods

Study population

This retrospective study has been approved by the Institutional Review Board (IRB). The study included patients with biochemically confirmed hyperparathyroidism who underwent multiphase 4DCT for localization parathyroid adenoma from Jan 2016 – June 2020. As for the inclusion of this study, patients had to have pathologically proven parathyroid adenoma or parathyroid hyperplasia or have Tc99m-sestamibi SPECT-CT confirmed hyperfunctioning parathyroid lesions. Exclusion criteria were: 1) small lesions for which accurate attenuation measurement on 4DCT could not be performed; 2) patients who do have a complete-three phase study; and, 3) images with severe artifact or noise over lower neck areas. Finally, 25 patients were recruited in this study: 18 female and 7 male patients (age range, 22 - 80 years; median 47 years). The types of hyperparathyroidism were as follows: primary hyperparathyroidism - 16 patients, and tertiary hyperparathyroidism - 9 patients. Ten patients had 1 lesion; 10 patients had 2 lesions; 3 patients had 3 lesions;and, 2 patients had 4 lesions. The total number of hyperfunctioning parathyroid lesions were 47. The locations of the lesions were as follows: right superior - 2 lesions (8.0%), right inferior - 8 lesions (32.0%), left superior - 7 lesions (28.0%), left inferior - 4 lesions (16.0%), and ectopic location - 4 lesions (16.0%). Tc99m-sestamibi SPECT-CT was available for 42 lesions. Tc99m-sestamibi SPECT-CT showed MIBI uptake in 36 lesions (86.0%) and no uptake in 6 lesions (14.0%). Pathology was available for 38 lesions (81.0%) (parathyroid hyperplasia 32 lesions and parathyroid adenoma 6 lesions).

Imaging acquisition

Imaging studies were performed using a 192 slice multidetector computed tomography (MDCT) scanner (SIEMENS, SOMATOM Force) and 64 slice MDCT scanner (GE discovery CT750 HD). The 192 slice MDCT images were obtained using the following parameters: 120 kV, reference mAs 116, 0.6 mm collimation, pitch factor 0.8 and gantry rotation time of 1 second. The 64 - slice MDCT images were obtained using the following parameters: 120 kV, automatic tube current modulation (100 - 500 mA), 0.6 mm collimation, pitch factor 0.516 and gantry rotation time of 0.5 second. Initially, non-contrast scans were obtained. The next two phases were performed after intravenous administration of 75 ml of nonionic contrast material (Iopamidol) at a rate of 4 ml/sec with a power injector at 25 seconds (A phase) and 80 seconds (D phase). The 0.6 mm thick contiguous axial images in all three phases were sent for interpretation.

Imaging analysis

Retrospective image analysis was performed by two radiologists who were not blinded to the pathologic results. The two reviewers included a neuroradiologist with 14 years of experience and a neuroradiology fellow with 4 years of experience. The two reviewers separately measured the attenuation in each patient by using labeled imaging localization conducted on 47 hyperfunctioning thyroid lesions, 22 thyroid glands (in 3 patients having undergone total thyroidectomy),

25 sternocleidomastoid muscle and 25 selected jugulodigastric lymph nodes. Multiple circular regions of interest (ROIs) were placed for measurement of the attenuation (Figure 1). The mean value from the two readers was used to represent attenuation of the lesions. The ROIs were made as large as possible while avoiding the lesion edges. Cystic or necrotic or calcified components were excluded from the ROI. The attenuation in Hounsfield Units (HU) were measured at non-contrast (NC), 25 seconds delayed (A phase) and 80 seconds delayed (D phase) scans. The ratio of attenuation of hyperfunctioning parathyroid lesions, lymph nodes and thyroid tissue to muscle in each phase were calculated.

The percentage changes in attenuation (and ratio of attenuation) of hyperfunctioning parathyroid lesions, lymph nodes and thyroid glands were calculated. The percentage change in attenuation from NC to A phase (arterial uptake percentage) was calculated by A-NC/NC x 100. The percentage change in attenuation from NC to D phase (delayed uptake percentage) was calculated by D-NC/NC x 100. The percentage change in attenuation from A phase to D phase (washout percentage) was calculated by A-D/A x 100.

Statistical analysis

Statistical analysis was performed by using software (SPSS; Statistical Package for the Social Sciences, IBM corporation). The demographic data and clinical information were summarized and analyzed by descriptive method. Mean and standard deviation (SD) of attenuation in the 3 phases, mean value of uptake percentage, and washout percentage were calculated to compare hyperfunctioning parathyroid lesions, lymph nodes and thyroid glands. Paired *t* - test was used to compare attenuation in the 3 phases, uptake percentage, and washout percentage between hyperfunctioning parathyroid lesions and lymph nodes and between hyperfunctioning parathyroid lesions and thyroid glands. The performance of attenuation in each phase, uptake percentage, and washout percentage to discriminate hyperfunctioning parathyroid lesions from lymph nodes and hyperfunctioning parathyroid lesions from thyroid glands was evaluated using receiver operating characteristic (ROC) curve analysis. ROC analysis was used to determine the optimal cut-off point. Subgroup analysis of two data sets were performed, one including all 47 lesions and the other including exclusively pathologically proven lesions.

Pearson correlation was used to determine correlation of parathyroid hormone level and percentage change in attenuation of hyperfunctioning parathyroid lesions. Interobserver reliability between the two radiologists was evaluated using the intraclass correlation coefficient (ICC). P - value < 0.05 was considered as statistically significant.

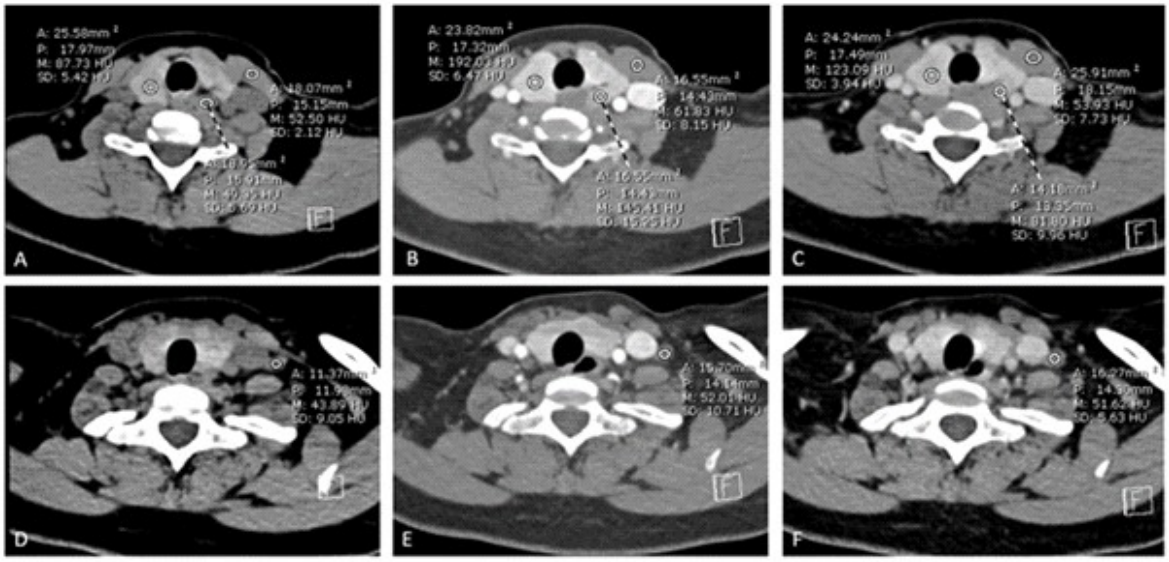

Figure 1. Circular regions of interest (ROIs) were placed for measurement of the attenuation of hyperfunctioning parathyroid lesions, thyroid glands, lymph nodes and muscles on non-contrast (A, D), arterial phase (B, E) and delay phase (C, F).

Results

Characterization of enhancement pattern of hyperfunctioning parathyroid lesions

Typical arterial uptake was observed with variable washout patterns from the arterial to delay phase of hyperfunctioning parathyroid lesions. Results revealed mostly mild washout (washout < 50.0%) (34 lesions, 72.0%), with a minority of the lesions showing washout > 50.0% (6 lesions, 13.0%). However, increased uptake from the arterial to delayed phase was detected in 7 lesions (15.0%).

In the 7 lesions that showed increased uptake from arterial to delayed phase; 4 lesions (8.5%) showed mild uptake from non-contrast to arterial phase (uptake < 100.0%) (a similar enhancement pattern to lymph nodes) and 3 lesions (6.4%) showed uptake from non-contrast to arterial phase > 100.0%. Six of 7 lesions had confirmed diagnosis by histopathology, except one with typical uptake on Tc99m-sestamibi SPECT-CT and 4DCT.

In the 40 lesions that showed washout from the arterial to delayed phase, the uptake percentage from non-contrast to arterial phase were as follows: < 100.0% in 3 lesions, 100.0 -200.0% in 11 lesions, 201.0 – 300.0% in 13 lesions, and > 300.0% in 13 lesions.

Attenuation in HU in non-contrast, arterial phase, delayed phase, percentage changes in attenuation (and ratio of attenuation), including arterial uptake percentage, delayed uptake percentage, and washout percentage were compared to differentiate hyperfunctioning parathyroid lesions and thyroid glands and differentiate hyperfunctioning parathyroid lesions and lymph node (Table 1) (Figure 2, 3).

Differentiation of hyperfunctioning parathyroid lesions and thyroid glands

Hyperfunctioning parathyroid lesions demonstrated significantly lower attenuation than thyroids in all 3 phases ($P < 0.001$) (Table 1) (Figure 2, 3). Percentage changes in attenuation (and ratio of attenuation), including arterial uptake percentage and delayed uptake percentage were significantly higher in hyperfunctioning parathyroid lesions ($P < 0.001$) (Table 1) (Figure 3 - 4). There was no significant difference in washout percentage; however, statistical significance was reached while using the washout percentage of ratio of attenuation (Table 1).

Table 1. Attenuation (HU) by time and percentage change of attenuation.

	Hyperfunctioning parathyroid lesion (P)	Thyroid gland (T)	Lymph node (L)	*P* - value	
				P *vs* T	P *vs* L
Non-contrast	53.84 (11.65)	97.42 (20.88)	54.06 (6.62)	< 0.001*	0.907
attenuation (HU)	54.52 (11.79)	96.82 (21.77)	53.97 (7.10)	< 0.001*	0.798
Arterial phase (25 sec)	172.33 (53.52)	208.56 (49.82)	81.90 (19.50)	0.001*	< 0.001*
attenuation (HU)	173.75 (52.65)	203.04 (48.89)	81.58 (20.69)	0.005*	< 0.001*
Delay phase (80 sec)	118.79 (25.95)	171.88 (33.59)	105.19 (20.63)	< 0.001*	0.001*
attenuation (HU)	119.46 (25.04)	169.41 (32.75)	104.83 (20.20)	< 0.001*	0.002*
% arterial uptake	232.77 (120.90)	124.84 (83.23)	52.95 (38.93)	< 0.001*	< 0.001*
	228.99 (114.15)	121.08 (86.70)	52.50 (40.48)	< 0.001*	< 0.001*
% delayed uptake	126.70 (52.07)	85.23 (60.81)	96.26 (40.10)	< 0.001*	< 0.001*
	125.05 (50.98)	84.04 (59.82)	95.82 (38.38)	0.001*	0.001*
% washout	24.96 (29.22)	13.73 (23.44)	- 33.51 (34.81)	0.072	< 0.001*
	26.10 (23.86)	12.36 (24.59)	- 34.88 (38.30)	0.027*	< 0.001*
% arterial uptake ratio	201.79 (105.09)	102.03 (64.09)	39.05 (33.53)	< 0.001*	< 0.001*
of attenuation	199.47 (100.97)	99.65 (66.38)	39.29 (34.95)	< 0.001*	< 0.001*
% delayed uptake ratio	87.55 (44.78)	51.23 (41.59)	61.89 (30.33)	< 0.001*	< 0.001*
of attenuation	87.45 (44.58)	52.55 (41.92)	63.70 (30.57)	0.001*	0.009*
% washout ratio of	61.65 (61.83)	21.64 (22.24)	- 20.44 (27.87)	0.001*	< 0.001*
attenuation	60.72 (53.73)	19.80 (23.30)	- 22.38 (30.56)	< 0.001*	< 0.001*

Values are presented as mean (SD). Values with * are statistically significant.
HU = Hounsfield units
The underlined values are from subgroup analysis of exclusively pathologically confirmed hyperfunctioning parathyroid lesions.

Differentiation of hyperfunctioning parathyroid lesions and lymph nodes

Hyperfunctioning parathyroid lesions demonstrated significantly higher attenuation compared with lymph nodes in the arterial phase and delayed phase ($P < 0.001$), but no significant difference was observed in the non-contrast phase (Table 1) (Figure 2, 3). Percentage changes in attenuation (and ratio of attenuation), including arterial uptake percentage, delayed uptake percentage, and washout percentage were significantly higher in hyperfunctioning parathyroid lesions ($P < 0.001$) (Table 1) (Figure 3 - 4).

ROC curve analysis and optimal cut-off value

Based on ROC curve analysis, the ability to differentiate hyperfunctioning parathyroid lesions from thyroid glands and to differentiate hyperfunctioning parathyroid lesions from lymph nodes revealed no significant difference between percentage change and percentage change from ratio of attenuation. The cut-off value of percentage change was used due to its simplicity for routine clinical practice.

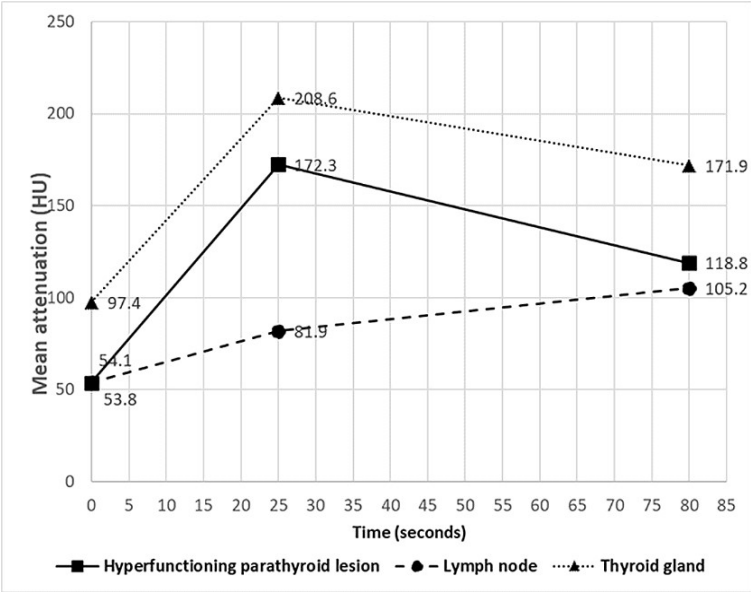

Figure 2. Mean of attenuation (HU) on non-contrast, arterial phase (25 sec) and delay phase (80 sec) of all included hyperfunctioning parathyroid lesions, thyroid glands and lymph nodes.

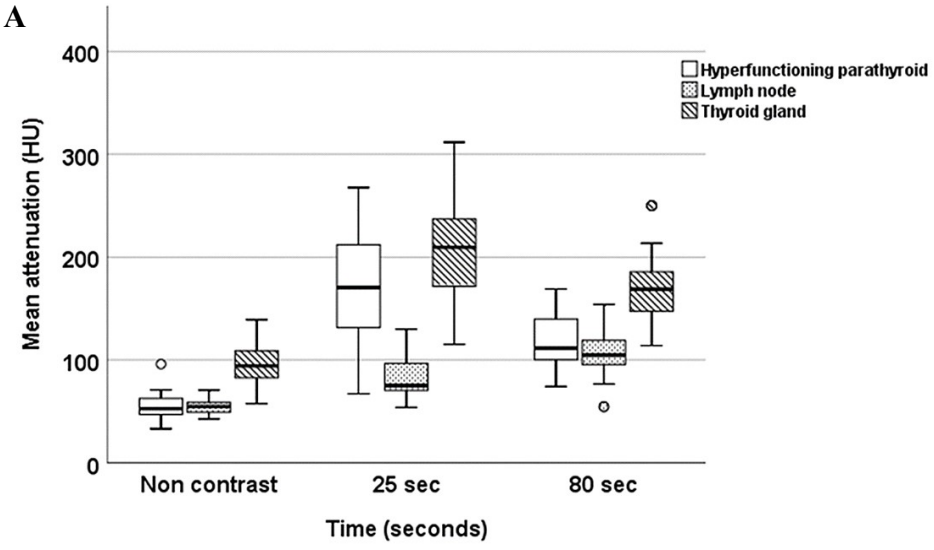

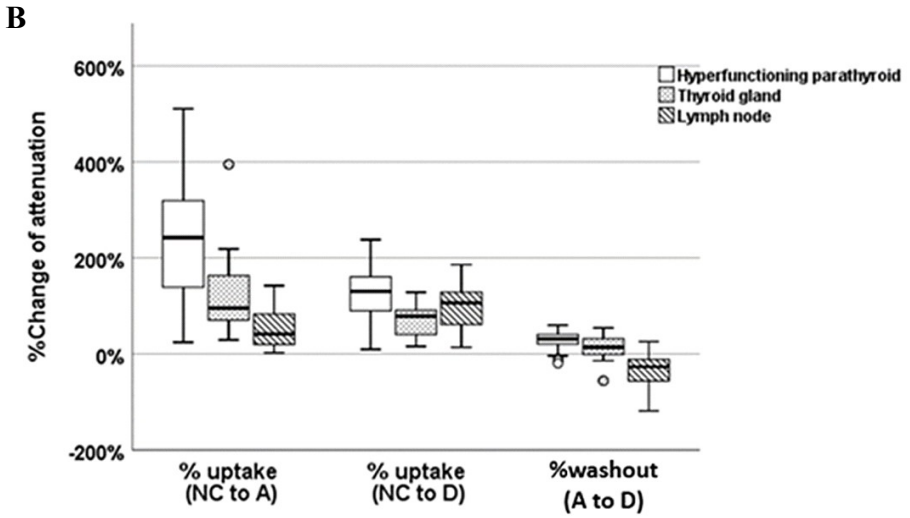

Figure 3. Box plot of HU measurements (A) and absolute percentage change (B) of all included hyperfunctioning parathyroid lesions, thyroid glands and lymph nodes on non-contrast, arterial phase (25 sec) and delay phase (80 sec).

ROC curve analysis of attenuation in 3 phases and percentage change to differentiate hyperfunctioning parathyroid lesions from thyroid glands showed that the area under the ROC curve was greatest in the non-contrast phase, followed by delayed

Table 2. ROC analysis for differentiation between hyperfunctioning parathyroid lesions and thyroid glands and lymph nodes.

	Hyperfunctioning parathyroid lesions and thyroid glands				Hyperfunctioning parathyroid lesions and lymph nodes			
	AUC	95% CI		*P*-value	AUC	95% CI		*P*-value
		Lower	Upper			Lower	Upper	
Non-contrast	0.972	0.939	1.000	<0.001*	0.495	0.375	0.616	0.937
	0.965	0.924	1.000	<0.001*	0.516	0.382	0.649	0.811
Arterial phase (25 sec)	0.674	0.563	0.785	0.005*	0.950	0.905	0.994	<0.001*
	0.643	0.516	0.770	0.037*	0.950	0.901	0.999	<0.001*
Delay phase (80 sec)	0.904	0.845	0.963	<0.001*	0.627	0.513	0.740	0.035*
	0.902	0.835	0.968	<0.001*	0.646	0.521	0.771	0.028*
% arterial uptake	0.775	0.676	0.873	<0.001*	0.940	0.896	0.984	<0.001*
	0.794	0.688	0.900	<0.001*	0.949	0.906	0.991	<0.001*
% delayed uptake	0.750	0.642	0.858	<0.001*	0.683	0.575	0.791	0.002*
	0.752	0.633	0.871	<0.001*	0.675	0.553	0.796	0.009*
% washout	0.687	0.575	0.799	0.002*	0.928	0.870	0.985	<0.001*
	0.693	0.569	0.818	0.005*	0.931	0.876	0.986	<0.001*
% arterial uptake ratio	0.779	0.683	0.876	<0.001*	0.938	0.888	0.988	<0.001*
of attenuation	0.790	0.686	0.894	<0.001*	0.952	0.910	0.994	<0.001*
% delayed uptake ratio	0.748	0.642	0.853	<0.001*	0.669	0.557	0.780	0.005*
of attenuation	0.730	0.610	0.849	0.001*	0.657	0.530	0.784	0.018*
% washout ratio of	0.760	0.651	0.870	<0.001*	0.890	0.816	0.964	<0.001*
attenuation	0.764	0.645	0.883	<0.001*	0.907	0.836	0.978	<0.001*

Values with * are statistically significant.
AUC = area under the ROC curve
The underlined values are from subgroup analysis of exclusively pathologically confirmed hyperfunctioning parathyroid lesions.

phase, arterial uptake percentage and delayed uptake percentage (Table 2) (Figure 4A).

The optimal cut-off value to differentiate all included 47 hyperfunctioning parathyroid lesions from thyroid glands by ROC analysis were as follows: non-contrast, ≤ 71.7 HU; delayed phase, ≤ 144.02 HU; arterial uptake percentage, ≥ 219.6%; delayed uptake percentage, ≥ 92.0% (Table 3). Similar results were calculated from the exclusively pathologically proven subgroup.

ROC curve analysis of attenuation in 3 phases and percentage change to differentiate hyperfunctioning parathyroid lesions from lymph nodes showed that the area under the ROC curve was greatest in the arterial phase, followed by arterial uptake percentage and washout percentage (Table 2, 4) (Figure 4B).

The optimal cut-off values to differentiate all included 47 hyperfunctioning parathyroid lesions from lymph nodes by ROC analysis were as follows: arterial phase, ≥ 107.09 HU; arterial uptake percentage,

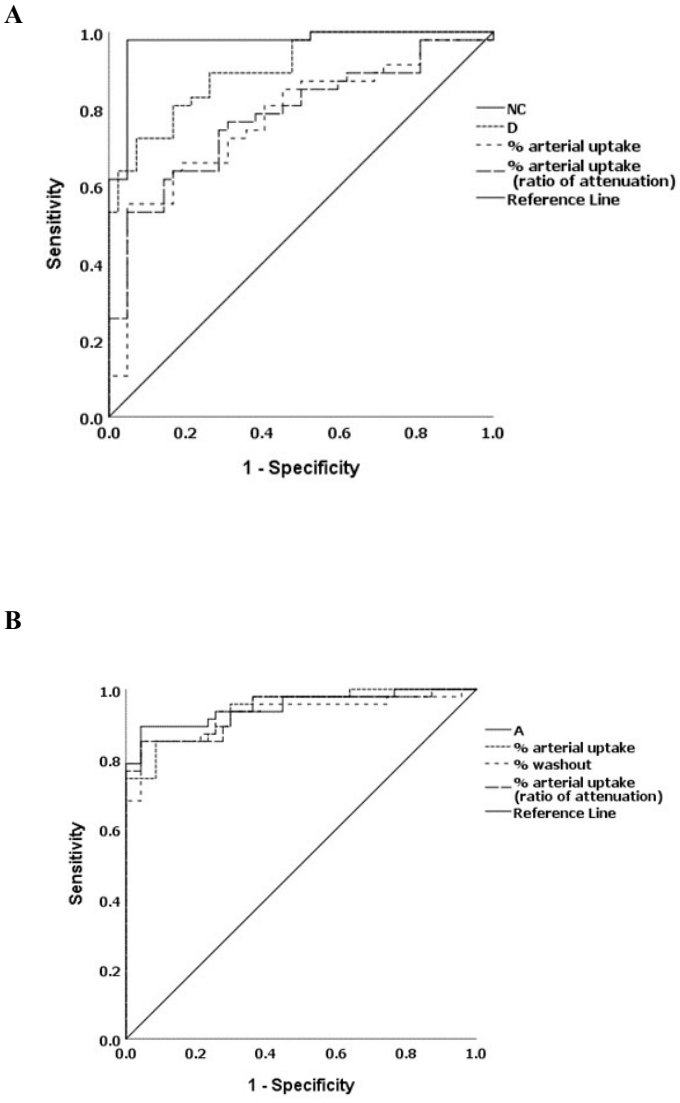

Figure 4 ROC plots comparing (A) all included hyperfunctioning parathyroid lesions and thyroid glands. The greatest area under the curve was in non-contrast followed by delay phase, arterial uptake percentage (ratio of attenuation) and arterial uptake percentage. (B) all included hyperfunctioning parathyroid lesions and lymph nodes.

Table 3. Areas under ROC curve and optimal cut-off value for differentiation between hype functioning parathyroid lesions and thyroid glands.

Phase	Optimal cut-off value	AUC	Sensitivity (%)	Specificity (%)	Accuracy (%)
Non-contrast attenuation (HU)	71.7	0.972	97.9	95.2	96.6
	71.7	0.965	97.4	94.1	95.8
Delay phase (80 sec) attenuation (HU)	144.0	0.904	80.9	83.3	82.0
	152.4	0.902	92.1	73.5	83.3
% arterial uptake	219.6	0.775	55.3	95.2	74.2
	169.3	0.794	65.8	85.3	75.0
% delayed uptake	92.0	0.750	72.3	78.6	75.3
	92.0	0.752	71.1	79.4	75.0

AUC = area under the ROC curve
HU = Hounsfield units
The underlined values are from subgroup analysis of exclusively pathologically confirmed hyperfunctioning parathyroid lesions.

Table 4. Areas under ROC curve and optimal cut-off value for differentiation between hyperfunctioning parathyroid lesions and lymph nodes.

Phase	Optimal cut-off value	AUC	Sensitivity (%)	Specificity (%)	Accuracy (%)
Arterial phase (25 sec) attenuation (HU)	107.1	0.950	89.4	95.7	92.6
	107.1	0.950	89.5	94.7	92.1
% arterial uptake	98.8	0.940	85.1	91.5	88.3
	98.6	0.949	86.8	89.5	88.2
% washout	10.1	0.928	85.1	95.7	90.4
	10.1	0.931	84.2	94.7	89.5

AUC = area under the ROC curve
HU = Hounsfield units
The underlined values are from subgroup analysis of exclusively pathologically confirmed hyperfunctioning parathyroid lesions.

≥ 98.8%; washout percentage, ≥ 10.1% (Table 4). Similar results were achieved from the exclusively pathologically proven subgroup.

Differentiation between hyperfunctioning parathyroid lesions, thyroid glands and lymph nodes is represented in diagram form (Figure 5).

Correlation of parathyroid hormone level and percentage change in attenuation of hyperfunctioning parathyroid lesions

There was no significant correlation between parathyroid hormone level and uptake and washout percentages of hyperfunctioning parathyroid lesions.

Interobserver reliability

The ICC shows moderate correlation for attenuation of muscle in A phase (0.71), good correlation for attenuation of lymph node in NC

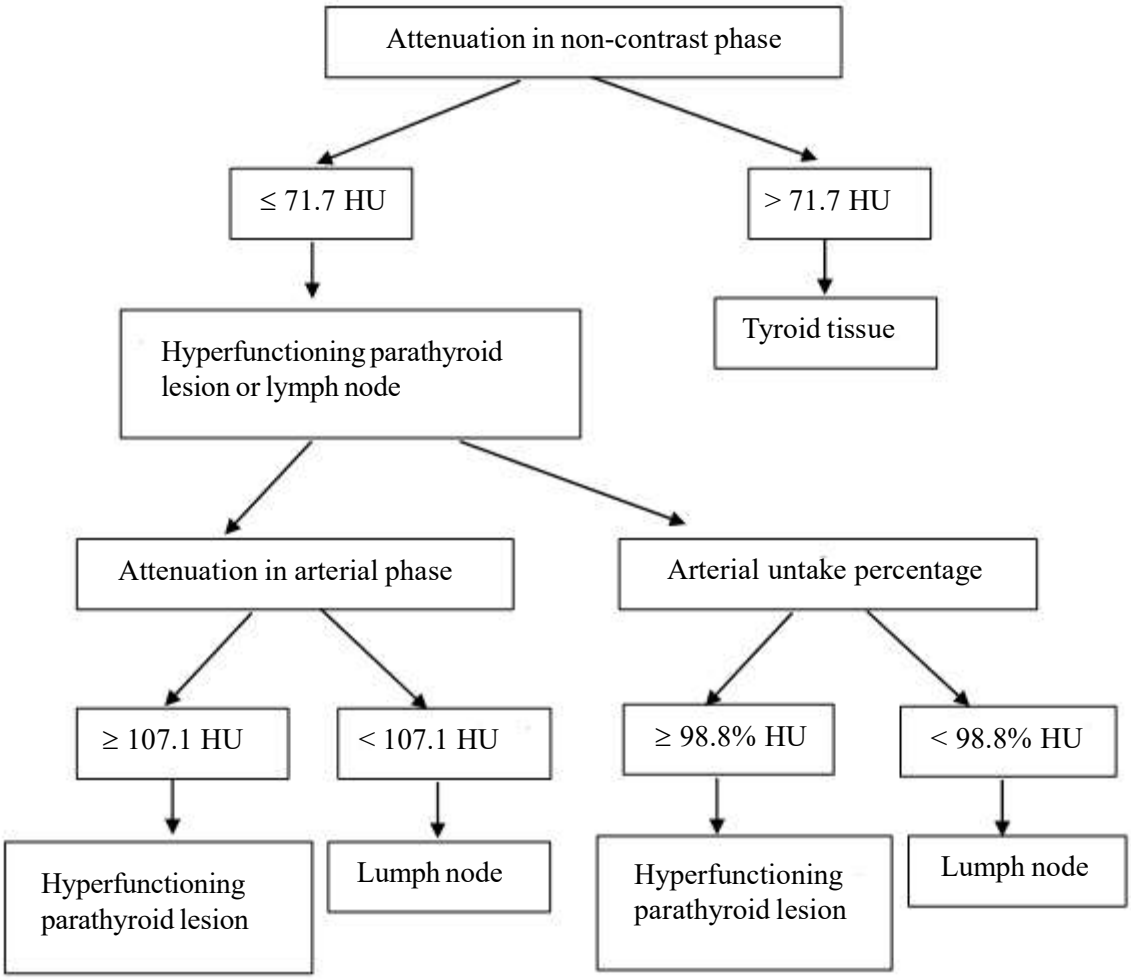

Figure 5. Diagram for differentiation between hyperfunctioning parathyroid lesions, thyroid glands and lymph nodes. (Data from all included hyperfunctioning parathyroid lesions).

(0.785), attenuation of muscle in NC and D phase (0.821, 0.821), attenuation of parathyroid lesion in NC (0.849) and excellent correlation of the other parameters (0.910 - 0.976) between the two radiologists.

Discussion

According to high specificity of Tc99m-sestamibi SPECT-CT, the results of subgroups analysis demonstrated similar values between all included hyperfunctioning parathyroid lesions and exclusively pathologically proven lesions. We believed that the data from all included lesions were more likely to reflect the routine clinical practice.

Our results demonstrate that quantitative measurement on 4DCT can be used to differentiate hyperfunctioning parathyroid lesions from thyroid glands and lymph nodes. Based on the ROC curve analysis, the best single phase to differentiate hyperfunctioning parathyroid lesions from thyroid glands was the non-contrast phase with high area under the ROC curve (0.97) with a cutoff value of ≤ 71.7 HU, yielding high sensitivity and specificity in both subgroups. The high electron density of the iodine colloid is attributed to the high attenuation of the normal thyroid tissue on MDCT.

While using quantitative measurement on multiphase, cut-off value of arterial uptake percentage of > 219.6% yielded 95.2% specificity to discriminate all hyperfunctioning parathyroid lesions from thyroid tissue in the 'fair' range for area under the ROC curve. This might be due to similar physiologic uptake of both thyroid glands and hyperfunctioning parathyroid lesions. We recommend using both non-contrast attenuation and arterial uptake percentage for better discrimination. However, functioning thyroid nodule or hot nodule which showed high arterial uptake percentage may mimic the pattern of hyperfunctioning parathyroid lesions, further investigation to differentiate these two entities is recommended.

Hyperfunctioning parathyroid lesions showed significantly higher attenuation compared with lymph nodes in the arterial phase and delay phase, but no significant difference in attenuation from the lymph node in the non-contrast phase. Based on the ROC curve analysis, the best single phase to differentiate hyperfunctioning parathyroid lesions from lymph nodes was the arterial phase with high area under the ROC curve (0.95) with a cut-off value of ≥ 107.09 HU, yielding high sensitivity and specificity in both subgroups.

While using quantitative multiphase measurement to differentiate all hyperfunctioning parathyroid lesions from lymph nodes, a cut-off value of arterial uptake of > 98.8% yielded 95.2% specificity with 'excellent' area under the ROC curve, and washout of > 10.1% yielded 95.7% specificity with 'excellent' area under the ROC curve. Simplification by using arterial uptake of > 100.0% and washout of > 10.0% might be more suitable for clinical practice.

Vu TH, *et al*. [17] performed quantitative analysis of enhancement patterns of 48 parathyroid adenomas with 4DCT, comparing them with normal thyroid tissue. Their results showed that parathyroid adenomas have a lower baseline density, higher arterial uptake percentage and higher washout percentage than thyroid tissue. The results in this study corresponded with the present study.

Bahl M, *et al*. [18] reviewed preoperative 4DCT scans in 94 patients with parathyroid adenomas or hyperplasia. They described three relative enhancement patterns of parathyroid adenoma comparing them with normal thyroid tissue on 4DCT. Type A lesions were higher in attenuation than the thyroid in the arterial phase, type B lesions were not higher in attenuation than the thyroid in the arterial phase but were lower in attenuation than the thyroid in the delayed phase, and type C lesions were neither higher in attenuation than the thyroid in the arterial phase nor lower in attenuation than the thyroid in the delayed phase. They found that type B enhancement was most common (57.0%), followed by type C (22.0%) and type A (20.0%). In our study, quantitative analysis showed that hyperfunctioning parathyroid lesions demonstrated significantly lower attenuation than thyroid glands in all 3 phases. It also revealed that the type B lesion was most common (66.0%), followed by type A (21.0%) and type C (13.0%). Further application of our quantitative cut-off value, specifically on type C lesions, which is the most difficult type to diagnose, should be studied.

Raghavan P, *et al*. [15] reviewed enhancement patterns of 29 patients with parathyroid adenomas, comparing them with lymph nodes. The results showed that, in the delay phase (80 seconds), the attenuation of parathyroid lesions approaches that of lymph nodes. In our study, the attenuation on the delayed phase did not approach that of lymph nodes. We found variable washout patterns in hyperfunctioning parathyroid lesions. Increased uptake from the arterial to delayed phase was detected in 7 lesions (15.0%), representing an atypical pattern.

Limitations of our study include the relatively small number of patients and retrospective nature of the study. Future work should include prospective clinical trials to test and validate our diagnostic criteria. Secondly, there is no pathology proven for every lesion type and some patients had thyroid enlargement with multiple thyroid nodules. However, uptake on Tc99m-sestamibi SPECT-CT images were well appreciated in the non-pathologically proven patients. No equivocal nodules were included. The previously reported sensitivity and specificity of Tc99m-sestamibi SPECT-CT was 75.0% and 99.0% respectively for single-gland diseases, and 31.0% and 96.0% respectively for multi-gland diseases (overall sensitivity and specificity was 58.0% and 99.0% respectively).[21] There were no significant differences in results from our subgroup analysis, which may represent the high specificity of the SPECT-CT. Thirdly, there were some limitations for accurate attenuation measurement by various artifacts in lower neck areas. Lastly, our results cannot be applied with ectopic location of hyperfunctioning parathyroid lesions or recurrent diseases after parathyroidectomy since there might be a difference in vascular supply. We believe that Tc99m-sestamibi SPECT-CT is the most appropriate tool in such cases.

Conclusion

Our study suggests that the best single phase to differentiate hyperfunctioning parathyroid lesions from thyroid glands and lymph nodes were non-contrast and arterial phases, respectively. Arterial uptake percentage was the best discriminator between hyperfunctioning parathyroid lesions from thyroid glands and lymph nodes, as hyperfunctioning parathyroid lesions showed a significantly higher uptake percentage.

Conflict of interest statement

Each of the authors has completed an ICMJE disclosure form. None of the authors declare any potential or actual relationship, activity, or interest related to the content of this article.

Data sharing statement

The present review is based on the reference cited. Further details, opinions, and interpretation are available from the corresponding authors on reasonable request.

References

1. Ahmad R, Hammond JM. Primary, secondary, and tertiary hyperparathyroidism. Otolaryngol Clin North Am 2004;37:701-13.
2. Pitt SC, Sippel RS, Chen H. Secondary and tertiary hyperparathyroidism, state of the art surgical management. Surg Clin North Am 2009;89:1227-39.
3. Udelsman R, Lin Z, Donovan P. The superiority of minimally invasive parathyroidectomy based on 1650 consecutive patients with primary hyperparathyroidism. Ann Surg 2011;25:585-91.
4. Wilhelm SM, Wang TS, Ruan DT, Lee JA, Asa SL, Duh QY, et al. The American Association of Endocrine Surgeons guidelines for definitive management of primary hyperparathyroidism. JAMA Surg 2016;151: 959-68.
5. Malinzak MD, Sosa JA, Hoang J. 4D-CT for detection of parathyroid adenomas and hyperplasia: state of the art imaging. Curr Radio Rep 2017;5:8.
6. Eslamy HK, Ziessman HA. Parathyroid scintigraphy in patients with primary hyperparathyroidism: 99mTc sestamibi SPECT and SPECT/CT. Radiographics 2008; 28:1461-76.
7. Johnson NA, Tublin ME, Ogilvie JB. Parathyroid imaging: technique and role in the preoperative evaluation of primary hyperparathyroidism. AJR Am J Roentgenol 2007; 188:1706-15.
8. Kuzminski SJ, Sosa JA, Hoang JK. Update in parathyroid imaging. Magn Reson Imaging Clin N Am 2018;26:151-66.
9. Bunch PM, Randolph GW, Brooks JA, George V, Cannon J, Kelly HR. Parathyroid 4D CT: What the surgeon wants to know. RadioGraphics 2020;40: 1383-94.
10. Chazen J, Gupta A, Dunning A, Phillips C. Diagnostic accuracy of 4D-CT for parathyroid adenomas and hyperplasia. AJNR Am J Neuroradiol 2012;33:429-33.
11. Hoang JK, Sung WK, Bahl M, Phillips CD. How to perform parathyroid 4D CT: tips and traps for technique and interpretation. Radiology 2014;270: 15-24.
12. Hunter GJ, Schellingerhout D, Vu TH, Perrier ND, Hamberg LM. Accuracy of four-dimensional CT for the localization of abnormal parathyroid glands in patients with primary hyperparathyroidism. Radiology 2012;264:789-95.
13. Randall GJ, Zald PB, Cohen JI, Hamilton BE. Contrast-enhanced MDCT characteristics of parathyroid adenomas. Am J Roentgenol 2009;193:W139-W43.
14. Hunter GJ, Ginat DT, Kelly HR, Halpern EF, Hamberg LM. Discriminating parathyroid adenoma from local mimics by using inherent tissue attenuation and vascular information obtained with four-dimensional CT: formulation of a multinomial logistic regression model. Radiology 2014;270:168-75.
15. Raghavan P, Durst C, Ornan D, Mukherjee S, Wintermark M, Patrie J, et al. Dynamic CT for parathyroid disease: are multiple phases necessary? Am J Neuroradiol 2014; 35:1959-64.
16. Beland MD, Mayo-Smith WW, Grand DJ, Machan JT, Monchik JM. Dynamic MDCT for localization of occult parathyroid adenomas in 26 patients with primary hyperparathyroidism. Am J Roentgenol 2011; 196:61-5.
17. Vu TH, Guha-Thakurta N, Harrell RK, Ahmed S, Kumar AJ, Johnson VE, et al. Imaging characteristics of hyperfunctioning parathyroid adenomas using multiphase multidectector computed tomography: a quantitative and qualitative approach. J Comput Assist Tomogr 2011;35:560-7.
18. Bahl M, Sepahdari AR, Sosa JA, Hoang JK. Parathyroid adenomas and hyperplasia on four-dimensional CT scans: three patterns of enhancement relative to the thyroid gland justify a three-phase protocol. Radiology 2015;277:454-62.
19. Gafton A, Glastonbury C, Eastwood J, Hoang JK. Parathyroid lesions: characterization with dual-phase arterial and venous enhanced CT of the neck. Am J Neuroradiol 2012; 33:949-52.
20. Goroshi M, Lila AR, Jadhav SS, Sonawane S, Hira P, Goroshi S, et al. Percentage arterial enhancement: An objective index for accurate identification of parathyroid adenoma/hyperplasia in primary hyperparathyroidism. Clin Endocrinol (Oxf) 2017; 87: 791-8.
21. Yeh R, Tay YKD, Tabacco G, Dercle L, Kuo JH, Bandeira L, et al. Diagnostic performance of 4D CT and sestamibi SPECT/CT in localizing parathyroid adenomas in primary hyperparathyroidism. Radiology 2019;291: 469-76.